PERGAMON

Computers and Structures 74 (2000) 41–50

Computers & Structures

www.elsevier.com/locate/compstruc

# A simple technique for calculating natural frequencies of geometrically nonlinear prestressed cable structures

A.S.K. Kwan*

*School of Engineering, University of Wales Cardiff, PO Box 917, Cardiff, CF2 1XH, UK*

Received 30 April 1998; accepted 18 November 1998

**Abstract**

A simple approach to calculating natural frequencies of geometrically nonlinear cable structures is presented. The stiffness matrix for a three-dimensional straight element is provided. The justification for the use of a linearized stiffness relationship is shown. Illustrative examples show that this simple element produces results comparable to theoretical and experimental results in the literature. © 1999 Elsevier Science Ltd. All rights reserved.

## 1. Introduction

Prestressed cable structures, and their continuous counterparts in membrane or fabric structures, are often perceived as architecturally elegant structural forms, particularly for large clear span coverings. The extremely low weight to plan area ratio of such structures, and the associated curved surfaces, often present cable and fabric structures as refreshing alternatives to the more common bulky rectangular forms. The use of prestressed mechanisms as structural forms also tends to give clients and the general public the impression of utilizing the most modern of available technology. However, the same three properties of low-weight, unusual curved surfaces, and nonlinear response to load, combine to form challenging problems to the structural engineer charged with ensuring a cable or fabric structure has safe dynamic characteristics, especially under wind loading. It is therefore noteworthy that while more cable and fabric structures are being built, there has not been a corresponding increase in the literature in this field.

As with the spirit of an earlier paper on static response of cable structures to load [9], the purpose of this paper is to present a simple but sufficiently accurate technique for calculating natural frequencies of cable structures. The technique is based on a large deformation approach, initially in the force method, and on discrete straight prestressed cable elements. The technique calls on no more than a modest understanding of mechanics and numerical techniques, and thus the approach would be suitably employed in introducing the engineering student to vibration of cable structures.

While the volume of research in this field is relatively small (see reviews in Refs. [1,7]), there have been several researchers in the last two decades and results from their work are later referred to. It is noteworthy however that while many workers have applied a range of analytical methods to the treatment of prestressed cable structures, the present author does not know of any instance where attention is paid to the fact that since prestressed cable structures have a significantly nonlinear static response to load, their corresponding dynamic behaviour is necessarily nonlinear.

Nonlinear vibration has several phenomena not found in linear vibration and, in particular, any displacement–time relationship is dependent on initial conditions. Thus different values of so-called "natural frequencies" can be obtained for a given system simply

* Fax: +44-1222-874-826.
*E-mail address:* kwan@cardiff.ac.uk (A.S.K. Kwan)

0045-7949/00/$ - see front matter © 1999 Elsevier Science Ltd. All rights reserved.
PII: S0045-7949(98)00318-6

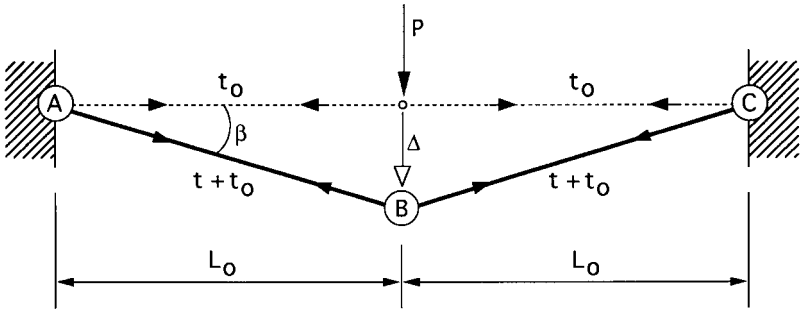


Fig. 1. A planar symmetrical two-link structure consisting of bars $AB$ and $BC$. Joint $B$ is displaced by $\Delta$ under load $P$.

by altering the initial velocity or displacement. Nonetheless, researchers in the literature on vibration of cable structures often employ a linear approach and therefore speak of "natural frequencies" without any further qualification, nor provision of a justification for the omission of higher order terms, except on the usual grounds of small deformation. We shall therefore begin this paper in the next section by examining this issue through the use of a simple two-link planar structure, with a view to setting up a definition of what we mean by "natural frequency" in a geometrically nonlinear cable structure.

The approach used for the two-link example can be readily extended and thus the derivation for a general three-dimensional element is given in Section 3, while illustrative examples are provided in Section 4 to verify the accuracy of this technique.

## 2. Nonlinear vibration of a two-link structure

Although the study of the vibration behaviour of prestressed cable networks should properly be a nonlinear treatment, we shall seek to show how information can be obtained without recourse to a full nonlinear analysis, and more importantly, to show the extent of the validity of the information we obtain in this way. For this, we shall examine the symmetrical prestressed two-link structure shown in Fig. 1 which has a single degree of freedom in $\Delta$. It can be shown [9] that a central load $P$ for this structure is related to its corresponding static deflection $\Delta$ by

$$\frac{EA}{L_0}\Delta^3 + 2t_0L_0\Delta - PL_0^2 = 0 \tag{1}$$

where $EA$ is the axial stiffness, $t_0$ is the initial pretension, and $L_0$ is the original undeformed length, of the two links.

Consider now the vibration of the two links such that they remain straight throughout, see Fig. 2, in which case the acceleration of a small element of length $\mathrm{d}x$ at a distance $x$ from the support is $x\Delta/L_0$, where $\Delta$ is the acceleration of joint $B$. The D'Alembert forces $D$ for one link are thus given by

$$D = \int_{x=0}^{x=L_0} \rho \mathrm{d}x\left(\frac{x}{L_0}\ddot{\Delta}\right) = \frac{\rho\ddot{\Delta}}{L_0}\int_0^{L_0} x\mathrm{d}x = \frac{\rho\ddot{\Delta}L_0}{2} \tag{2}$$

where $\rho$ is the mass per unit length of the links. If we isolate the portion $BC$, and take free body moment of the portion $BC$ about $B$, we obtain

$$\int_{x=0}^{x=L_0} \rho \mathrm{d}x\left(\frac{x}{L_0}\ddot{\Delta}\right)(L_0 - x) = RL_0$$

$$\frac{\rho\ddot{\Delta}L_0}{6} = R \tag{3}$$

where $R$ is the vertical dynamic reaction at the supports. Substitution of Eqs. (1)–(3) into the overall vertical equilibrium relationship $R = P/2 + D$ leads to

$$\ddot{\Delta} + \frac{3t_0}{\rho L_0^2}\Delta + \frac{3EA}{2\rho L_0^4}\Delta^3 = 0 \tag{4a}$$

which is the equation describing the free undamped vibration of the prestressed two-link. If the two link structure had a concentrated mass $M$ at $B$, then Eq. (4a) would be altered slightly to

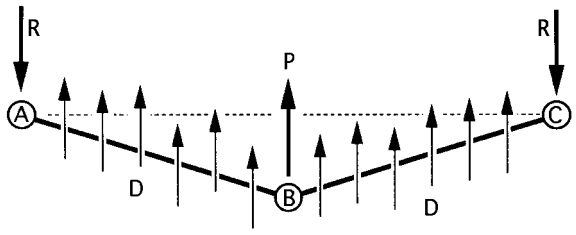


Fig. 2. Equilibrium of the dynamic forces on the vibrating two-link structure.

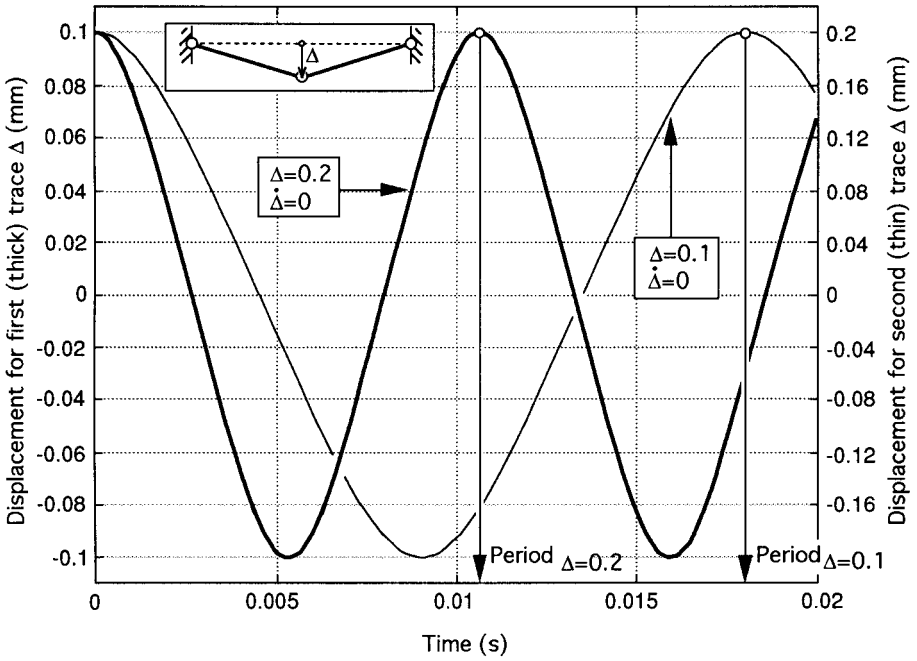


Fig. 3. Displacement-time plot for the two-link structure for initial displacements of 0.1 and 0.2 mm. Note that the displacement scale (but not the time scale) for the second plot has been halved.

$$\ddot{\Delta} + \frac{6t_0}{3ML_0 + 2\rho L_0^2}\Delta + \frac{3EA}{3ML_0^3 + 2\rho L_0^4}\Delta^3 = 0 \qquad (4b)$$

It is interesting to note in passing that the linear terms in both Eqs. (4a) and (4b) are dependent only on the prestress $t_0$ and completely independent of the axial stiffness. Therefore, where the amplitude of oscillation is small, and hence where the $\Delta^3$ term can be neglected, the natural frequency is controlled by the level of prestress, rather than the stiffness of the structural system.

Displacement–time plots for Eq. (4), taking into account both linear and cubic terms, can be simply obtained from a Runge–Kutta numeric integration, as seen in Fig. 3 for $EA = 556$ kN, $L_0 = 1.143$ m, $\rho = 4.6415 \times 10^{-2}$ kg/m, $t_0 = 3558.6$ N and $M = 0$. Two traces are shown in Fig. 3 for the two different initial displacements of 0.1 and 0.2 mm; there is no initial velocity in either case. Although both traces are for exactly the same structure with exactly the same prestress, the period of oscillation is clearly different. As the initial displacement decreases, the corresponding free vibration period increases. This relationship however, is not linear but asymptotic; there is a limiting value for the period.

Closed-form expression for the period of oscillation described in Eq. (4) can in fact be obtained with simple integrals. Let Eq. (4) be re-written as

$$\ddot{\Delta} + \alpha\Delta + \beta\Delta^3 = 0 \quad \text{i.e.} \quad \dot{\Delta}\frac{d\dot{\Delta}}{d\Delta} + \alpha\Delta + \beta\Delta^3 = 0$$

which, when integrated with respect to $\Delta$, gives

$$\dot{\Delta}^2 + \alpha\Delta^2 + \frac{\beta\Delta^4}{2} = 2E \qquad (5)$$

in which the constant of integration $E$ is the total energy in the two-link structure. In the vicinity of the origin of the phase plot, where $\Delta \approx \dot{\Delta} \approx 0$, these energy curves take the form of closed ellipses because the fourth-order term would be insignificant in comparison to the second-order term. The maximum displacement occurs as the velocity turns zero and hence

$$\Delta_{\max}^2 = \frac{-\alpha + \sqrt{\alpha^2 + 4\beta E}}{\beta}$$

The period of oscillation can be obtained from line integral along an energy curve. Since we are still within the vicinity of the origin, and therefore still in the realms of closed energy ellipses, we need only integrate a quarter of an ellipse. The period is thus

$$T = \oint \mathrm{d}t = \oint \frac{\mathrm{d}\Delta}{\dot{\Delta}} = 4\int_0^{\Delta_{\max}} \frac{\mathrm{d}\Delta}{\sqrt{2E - \alpha\Delta^2 - \dfrac{\beta\Delta^4}{2}}} \qquad (6)$$

The integral in Eq. (6) is actually more instructive

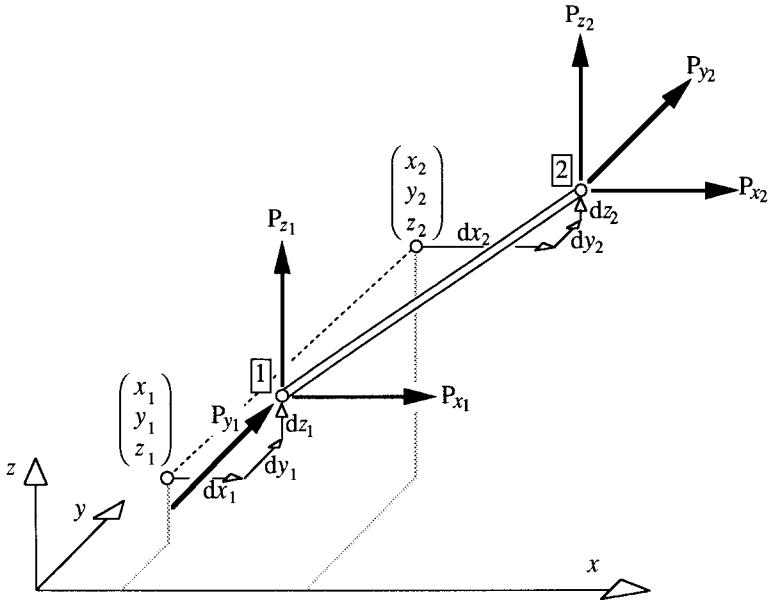


Fig. 4. Loads and displacements on the 3D element.

when the substitution $\Delta = \Delta_{max}\sin\theta$ is made (i.e. in radial coordinates),

$$T = 4\sqrt{2}\int_0^{\pi/2} \frac{d\theta}{\sqrt{2\alpha + \beta\Delta_{max}\,(1+\sin^2\theta)}} \tag{7}$$

because we can now clearly see that the period is amplitude dependent, as we have discovered in Fig. 3. It follows from amplitude dependent frequency that the term "natural frequency" can therefore not take its usual meaning; we should only use the term in the usual way after we have defined the amplitude.

We have already remarked earlier when examining Fig. 3 that there is a limiting value for period with decreasing amplitude. It would seem that the only sensible definition for "natural frequency" would be that asymptotic frequency associated with infinitesimal amplitude. With $\Delta_{max} \to 0$, the $\beta$ term in Eq. (7) would become ineffectual. That is, as the amplitude tends to zero, the period for nonlinear vibration tends to that for the equivalent linearized vibration and this is completely independent of the size of the nonlinearity in the system. Here then is the justification for the removal of higher order terms that is not, to the author's knowledge, found in the literature.

The removal of $\beta$ would reduce Eq. (4b) to

$$\ddot{\Delta} + \frac{6t_0}{3ML_0 + 2\rho L_0^2}\Delta = 0 \tag{8}$$

and, by inspection, the natural frequency is

$$\omega = \frac{1}{2\pi}\sqrt{\frac{6t_0}{3ML_0 + 2\rho L_0^2}} \tag{9}$$

We shall return to Eq. (9) in the Section 4.

## 3. A three-dimensional-element

The justification for the removal of nonlinear stiffness terms in the calculation of the period of nonlinear vibration is fundamental in the establishment of a simple technique to assess the natural frequencies of three-dimensional cable structures. A simple, but thoroughly sufficient, geometrically nonlinear stiffness matrix, and the associated distributed mass matrix shall be derived in this section for a three-dimensional *straight* axial element. Although it has been argued that curved elements are necessary [3], it shall be shown that the element derived in this paper is entirely adequate even for examples without concentrated mass/loads.

The stiffness relationship for the three-dimensional element shown in Fig. 4 is based on the following relationships originally formulated in the flexibility method. These relationships are completely analogous to those for a two-dimensional geometrically nonlinear element shown previously by the author [9] so no detailed derivation will be provided here.

The internal bar tension $t$ of a bar of length $L$, with coordinates $(x_i,\ y_i,\ z_i)_{i=1,2}$ for its ends, is related to the external displacements through a consideration of

compatibility by:

$$t = \frac{EA}{L}\left\{\frac{\tilde{x}}{L}\mathrm{d}\tilde{x} + \frac{\tilde{y}}{L}\mathrm{d}\tilde{y} + \frac{\tilde{z}}{L}\mathrm{d}\tilde{z} + \left(\frac{1}{2L} - \frac{\tilde{x}^2}{2L^3}\right)\mathrm{d}\tilde{x}^2 + \left(\frac{1}{2L} - \frac{\tilde{y}^2}{2L^3}\right)\mathrm{d}\tilde{y}^2 + \left(\frac{1}{2L} - \frac{\tilde{z}^2}{2L^3}\right)\mathrm{d}\tilde{z}^2 - \frac{\tilde{x}\tilde{y}}{L^3}\mathrm{d}\tilde{x}\mathrm{d}\tilde{y} - \frac{\tilde{x}\tilde{z}}{L^3}\mathrm{d}\tilde{x}\mathrm{d}\tilde{z} - \frac{\tilde{y}\tilde{z}}{L^3}\mathrm{d}\tilde{y}\mathrm{d}\tilde{z}\right\} \tag{10}$$

where $\tilde{x} = x_2 - x_1$, $\mathrm{d}\tilde{x} = \mathrm{d}x_2 - \mathrm{d}x_1$, etc. The material here is assumed to have a linear response to load at all load levels. The equilibrium equations, which are derived in the displaced configuration are:

$$P_{x_2} = (t + t_0)\left\{\frac{\tilde{x}}{L} - \frac{\tilde{x}^2}{L^3}\mathrm{d}\tilde{x} - \frac{\tilde{x}\tilde{y}}{L^3}\mathrm{d}\tilde{y} - \frac{\tilde{x}\tilde{z}}{L^3}\mathrm{d}\tilde{z} + \frac{\mathrm{d}\tilde{x}}{L}\right\}$$

$$P_{y_2} = (t + t_0)\left\{\frac{\tilde{y}}{L} - \frac{\tilde{x}\tilde{y}}{L^3}\mathrm{d}\tilde{x} - \frac{\tilde{y}^2}{L^3}\mathrm{d}\tilde{y} - \frac{\tilde{y}\tilde{z}}{L^3}\mathrm{d}\tilde{z} + \frac{\mathrm{d}\tilde{y}}{L}\right\}$$

$$P_{z_2} = (t + t_0)\left\{\frac{\tilde{z}}{L} - \frac{\tilde{x}\tilde{z}}{L^3}\mathrm{d}\tilde{x} - \frac{\tilde{y}\tilde{z}}{L^3}\mathrm{d}\tilde{y} - \frac{\tilde{z}^2}{L^3}\mathrm{d}\tilde{z} + \frac{\mathrm{d}\tilde{z}}{L}\right\} \tag{11a}$$

and

$$P_{x_1} = -P_{x_2},\ P_{y_1} = -P_{y_2} \quad \text{and} \quad P_{z_1} = -P_{z_2} \tag{11b}$$

Here the prestress in the bar is denoted again by $t_0$. Substitution of $t$ from Eq. (10) to Eq. (11) leads to the set of load–displacement relationships, which when linearised, is

$$\begin{pmatrix} P_{x_1} \\ P_{y_1} \\ P_{z_1} \\ P_{x_2} \\ P_{y_2} \\ P_{z_2} \end{pmatrix} = \begin{pmatrix} \tilde{x}^2G + t_0/L & \tilde{x}\tilde{y}G & \tilde{x}\tilde{z}G & -\tilde{x}^2G - t_0/L & -\tilde{x}\tilde{y}G & -\tilde{x}\tilde{z}G \\ & \tilde{y}^2G + t_0/L & \tilde{y}\tilde{z}G & -\tilde{x}\tilde{y}G & -\tilde{y}^2G - t_0/L & -\tilde{y}\tilde{z}G \\ & & \tilde{z}^2G + t_0/L & -\tilde{x}\tilde{z}G & -\tilde{y}\tilde{z}G & -\tilde{z}^2G + t_0/L \\ & & & \tilde{x}^2G + t_0/L & \tilde{x}\tilde{y}G & \tilde{x}\tilde{z}G \\ & \text{sym.} & & & \tilde{y}^2G + t_0/L & \tilde{y}\tilde{z}G \\ & & & & & \tilde{z}^2G + t_0/L \end{pmatrix} \begin{pmatrix} \mathrm{d}x_1 \\ \mathrm{d}y_1 \\ \mathrm{d}z_1 \\ \mathrm{d}x_2 \\ \mathrm{d}y_2 \\ \mathrm{d}z_2 \end{pmatrix} + \begin{pmatrix} -t_0\tilde{x}/L \\ -t_0\tilde{y}/L \\ -t_0\tilde{z}/L \\ t_0\tilde{x}/L \\ t_0\tilde{y}/L \\ t_0\tilde{z}/L \end{pmatrix} \tag{12}$$

where $G = EA/2L^3$.

The distributed mass matrix is best formulated through Lagrange's equation. The kinetic energy $T$ for the 3D-element is

$$T = \int_{\zeta=0}^{\zeta=L_0} \frac{1}{2} m \mathrm{d}\zeta \left\{\frac{\zeta}{L_0}(\mathrm{d}\dot{x}_2 + \mathrm{d}\dot{y}_2 + \mathrm{d}\dot{z}_2) + \frac{L_0 - \zeta}{L_0}(\mathrm{d}\dot{x}_1 + \mathrm{d}\dot{y}_1 + \mathrm{d}\dot{z}_1)\right\}^2.$$

Individual rows of the mass matrix are obtained from

$$\frac{\mathrm{d}}{\mathrm{d}t}\frac{\partial T}{\partial(\mathrm{d}x_1)}, \frac{\mathrm{d}}{\mathrm{d}t}\frac{\partial T}{\partial(\mathrm{d}y_1)} \text{ etc.}$$

which leads to the mass matrix

$$\frac{mL_0}{6}\begin{pmatrix} 2 & 2 & 2 & 1 & 1 & 1 \\ 2 & 2 & 2 & 1 & 1 & 1 \\ 2 & 2 & 2 & 1 & 1 & 1 \\ 1 & 1 & 1 & 2 & 2 & 2 \\ 1 & 1 & 1 & 2 & 2 & 2 \\ 1 & 1 & 1 & 2 & 2 & 2 \end{pmatrix} \tag{13}$$

Where required, the usual lumped mass matrix $(mL_0/2)\mathbf{I}_{6\times 6}$, where $\mathbf{I}_{6\times 6}$ is the $6 \times 6$ identity matrix, could be used instead of Eq. (13).

## 4. Illustrative examples

Illustrative examples have been chosen for comparison to firstly show the technique chosen for dealing with the stiffness relationship and mass matrix, and secondly to show accuracy with results in the literature.

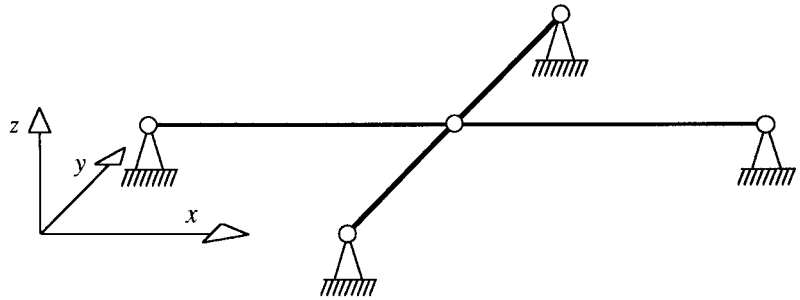


Fig. 5. A square flat net with each element having length of 1.143 m.

### 4.1. Example 1: 2 × 2 flat net

The first example is a small four cable flat net shown in Fig. 5. This structure has essentially only one single degree of freedom, and its natural frequency is identical to that of the two-link structure discussed in Section 3 and so, in addition to external literature, Eq. (9) can also be used to compare with results obtained with the formulae given in Section 3. We shall consider the case of $t_0 = 4448$ kN in detail.

Substituting the geometric and material parameters into Eqs. (12) and (13), together with an application of transformation matrix on the mass matrix, results in the following set of equations:

$$7.0736 \times 10^{-2} \begin{pmatrix} 1 & 0 & 0 \\ 0 & 1 & 0 \\ 0 & 0 & 1 \end{pmatrix} \begin{pmatrix} \mathrm{d}\ddot{x} \\ \mathrm{d}\ddot{y} \\ \mathrm{d}\ddot{z} \end{pmatrix} + \begin{pmatrix} 9.8071 \times 10^5 & 0 & 0 \\ 0 & 9.8071 \times 10^5 & 0 \\ 0 & 0 & 1.5567 \times 10^4 \end{pmatrix} \begin{pmatrix} \mathrm{d}x \\ \mathrm{d}y \\ \mathrm{d}z \end{pmatrix} = \begin{pmatrix} 0 \\ 0 \\ 0 \end{pmatrix} \quad (14)$$

i.e. $\mathbf{M}\ddot{\Delta} + \mathbf{K}\Delta = \mathbf{T}$

where the displacements and accelerations are those for the central unsupported joint. As it turned out in the above example, the mass and the stiffness matrices are both diagonal matrices and hence the natural frequencies can be obtained by a trivial division of the two diagonals; e.g. $\sqrt{(1.5567 \times 10^4 / 7.0736 \times 10^{-2})}$ gives 469.12 rad/s, i.e. 74.66 Hz.

In general, $\mathbf{M}\Delta + \mathbf{K}\Delta = \mathbf{T}$ would need to be uncoupled by the matrix of eigenvectors of the corresponding homogeneous equations $\mathbf{P}$ through $\mathbf{P}^{\mathrm{T}}\mathbf{M}\mathbf{P}\Delta + \mathbf{P}^{\mathrm{T}}\mathbf{K}\mathbf{P}\Delta = \mathbf{P}^{\mathrm{T}}\mathbf{T}$. Since such a transformation is purely a coordinate re-orientation, the natural frequencies would be unaltered by the transformation. The natural frequencies are found thereafter from the division of the two diagonals as above. Table 1 shows the variation of the fundamental natural frequency with pretension for the 2 × 2 flat net, as compared with results in the literature.

For comparison with the lumped-mass results given by Sangster [13], the present 3D element can be used with the lumped mass matrix. There is almost no discernible difference between the two sets of results. The experimentally measured results, as well as the membrane model results are also due to Sangster [13]. These were compared by Gambhir and Batchelor [4] who promoted their own curved finite element to improve on accuracy of finite elements that employed straight cable elements. Chisalita [2] developed com-

Table 1
Comparison of the fundamental frequency of the 2 × 2 flat net (Fig. 4) by various methods for different levels of pretension (1)lb = 4.44822 N)

| $t_0$ (lbs) | Lumped mass (Sangster) | Present lumped mass | Membrane model (Sangster) | Curved FE (Gambhir and Batchelor) | Measured (Sangster) | Closed form (Eq. (9)); present distributed mass; & Chisalita |
|---|---|---|---|---|---|---|
| 200 | 27.27 | 27.26 | 30.29 | 30.28 | 34 | 33.39 |
| 400 | 38.57 | 38.56 | 42.83 | 42.82 | 44 | 47.22 |
| 600 | 47.24 | 47.22 | 52.46 | 52.44 | 56 | 57.83 |
| 800 | 54.54 | 54.53 | 60.58 | 60.55 | 64 | 66.78 |
| 1000 | 60.98 | 60.96 | 67.73 | 67.70 | 73 | 74.66 |

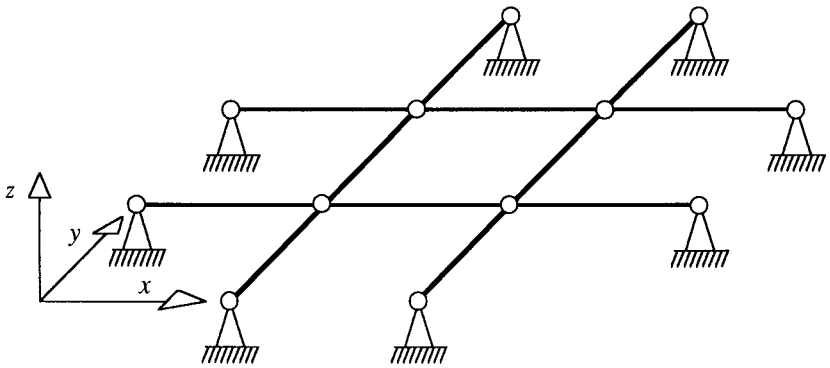


Fig. 6. A square flat net with each element having length of 1.016 m.

plex equations for cable networks that incorporated features such as large deformations with Poisson effect, elasto-plastic material properties, cable slack, and Piola–Kirchhoff stresses. In actual fact, for this simple example, Chisalita's formulation is reduced to Eq. (9), and hence Chisalita's results, Eq. (9), and the present 3D element with distributed mass (Eq. (13)) all produce the same results.

It is clear that the two lumped mass approaches produced consistently low frequencies and highlight the drawback of keeping the mass matrix diagonal. Gambhir and Batchelor's curved element was particularly successful in replicating the membrane model, but both techniques do not show a good match with the experimental results. Results from the current studies, and Chisalita's studies, both of which impose straight elements, correspond much better to Sansgter's experimental results, tending to dispute Gambhir and Batchelor's assumption that curved elements are necessarily better models for prestressed cable networks, particularly when this example was one without concentrated mass/loads at the joints.

### 4.2. Example 2: $3 \times 3$ flat net

The second example is a $3 \times 3$ flat net made up of cables with $EA = 44.48$ kN, $\rho = 2.589$ kg/m, and $t_0 = 333.62$ kN, see Fig. 6. This grid has previously been analysed by numerous researchers and the fundamental frequency from the present study is compared with results in the literature in Table 2. Leonard [10] used curved finite elements and analysed this net with three levels of discretisation. Again, it can be seen that the present technique produces very similar results to those in the literature, including those that employed curved elements.

### 4.3. Example 3: cable beam

The third example is a "cable beam" first introduced by Jensen [6] who produced experimental and theoretical results. The main cables have $EA = 190{,}314$ N, and vertical hangars have $EA = 103{,}005$ N. The cable geometry and initial cable tensions take values measured by Jensen, and these are shown in Fig. 7. Both Morris [11] and Chisalita [2] also analysed this example. The first few natural frequencies, and the range of natural frequencies where known, are presented in Table 3 for three load cases. Since concentrated loads are applied at the nodes, the present analysis and that by Chisalita have used the lumped

Table 2
Comparison of the fundamental frequency of the $3 \times 3$ flat net (Fig. 5) by various methods

| Method of analysis | Frequency (Hz) | |
|---|---|---|
| | Lumped | Distributed |
| Soler and Afshari [16]: | | |
| Galerkin | | 59.10 |
| Shore and Chaudhari [15]: | | |
| Lumped mass | 56.40 | |
| Membrane | | 58.80 |
| Leonard [10], finite element: | | |
| 12 elements | | 61.59 |
| 24 elements | | 59.55 |
| 48 elements | | 59.05 |
| Sangster and Batchelor [14]: | | |
| Lumped mass | 56.76 | |
| Equiv. Membrane | | 60.43 |
| Gambhir and Batchelor [3]: | | |
| Curved element | | 60.06 |
| Ozdemir [12], curved elements: | | |
| 2 node elements | | 61.64 |
| 3 node elements | | 58.97 |
| 4 node elements | | 58.93 |
| Present study (12 elements): | | |
| Lumped mass | 56.29 | |
| Distributed mass | | 61.37 |

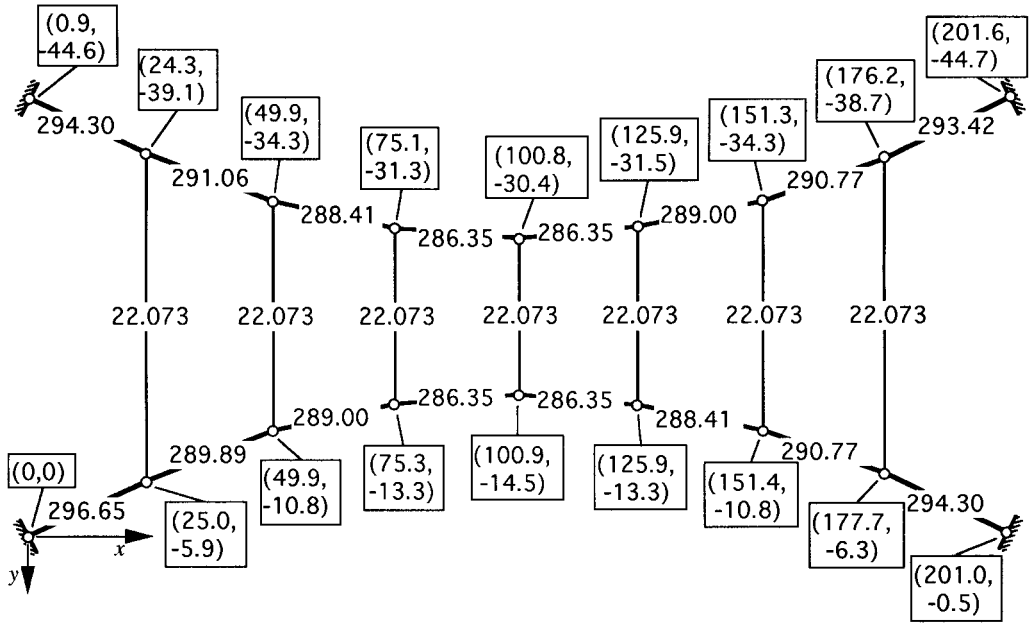


Fig. 7. Jensen's planar cable beam with coordinates (boxed values) in cm, and initially measured cable pretension in kN.

mass model. It can be seen that all theoretical results in this example are in good agreement with Jensen's experimental results, and the present study agrees closely with Chisalita's results even for $\omega_{28}$.

### 4.4. Example 4: Aden Airways building

The fourth example is a $35.052 \times 35.052$ m hyperbolic paraboloid, first presented by Knudson [8] as the Aden Airways building, having the shape function (m):

$$y = \frac{5.334}{17.526^2} z^2 - \frac{3.81}{17.526^2} x^2$$

and seven cables each way in equal spacings. The cables have $EA = 210.312$ MN, $\rho = 10.0$ kg/m, and horizontal component of cable prestress tension as 200.17 kN for cables in the $x$-direction, and 142.97 kN

Table 3
Measured and theoretically predicted natural frequencies for the cable beam tested by Jensen, under three load cases as detailed in Table 4

| | Case A | | | | | Case B | | | | Case C | |
|---|---|---|---|---|---|---|---|---|---|---|---|
| | Jensen, experimental | Jensen, theoretical | Morris, theoretical | Chisalita, theoretical | Present study | Jensen, experimental | Jensen, theorectical | Chisalita, theoretical | Present study | Chisalita, theoretical | Present study |
| $\omega_1$ | 5.7 | 5.78 | 5.82 | 5.698 | 5.683 | 7.50 | 8.07 | 8.077 | 8.077 | 5.773 | 5.768 |
| $\omega_2$ | 8.1 | 8.08 | 8.10 | 7.999 | 8.009 | 11.1 | 11.26 | 11.354 | 11.382 | 8.131 | 8.124 |
| $\omega_3$ | 10.9 | 10.51 | 10.51 | 10.423 | 10.402 | 14.5 | 14.65 | 14.785 | 14.781 | 10.593 | 10.569 |
| $\omega_4$ | 12.1 | 12.02 | 12.03 | 11.918 | 11.905 | 16.1 | 16.75 | 16.927 | 16.918 | 12.114 | 12.103 |
| $\omega_5$ | 12.8 | 12.81 | 12.81 | 12.896 | 12.922 | 17.2 | 17.87 | 18.315 | 18.363 | 13.136 | 13.127 |
| $\omega_6$ | 13.9 | 13.81 | | 13.757 | 13.826 | 19.1 | 19.27 | 19.541 | 19.648 | 14.033 | 14.026 |
| $\omega_7$ | 15.0 | 14.90 | | 14.728 | 14.720 | 21.0 | 20.70 | 20.919 | 20.918 | 14.986 | 14.970 |
| $\omega_8$ | | | | 54.206 | 54.275 | | | 76.694 | 76.778 | 74.212 | 74.221 |
| ⋮ | | | | ⋮ | ⋮ | | | | ⋮ | ⋮ | ⋮ |
| $\omega_{28}$ | | | 1565 | 1558.5 | 1557.5 | | | | 2697.7 | 382.10 | 382.16 |

Table 4
The distribution of mass for the three cases in Table 3

| | Case A | Case B | Case C |
|---|---|---|---|
| Mass on upper joints (kg) | 0.03 | 0.01 | 0.50 |
| Mass on lower joints (kg) | 1.00 | 0.50 | 0.50 |

for cables in the $z$-direction. The structure has 75 degrees of freedom.

The structure was initially analysed by Geshwinder and West [5], and then by Swaddiwudhipong et al. [17], both using a lumped mass model, see Table 5. Chisalita also provided results using a lumped mass which agree closely to those from the present study, and from Geshwinder and West, even for the last natural frequency. Swaddiwudhipong's set of results stands out as the one that is about 1% below the rest.

Chisalita also provided some results for the Aden building using a distributed mass model which the present study has failed to replicate, except for the fundamental natural frequency. The largest natural frequency quoted by Chisalita is 2286 rad/s, but the present study gives a value of around 15,700 rad/s. Chisalita's first four natural frequencies increased in almost constant steps, while the present study has found the second and third natural frequencies close to each other, a feature also seen in the lumped mass model. The present study would conclude with Chisalita though that "in order to find the correct values of the frequencies, a distributed mass model has to be adopted, the lumped mass model leading to lower values."

## 5. Conclusions

It can be concluded that the geometrically nonlinear axial element presented in this paper, together with the simple and quick frequency assessment procedure illustrated in Section 4, gives rapid and accurate answers. This study also questions the assumption that curved elements are necessarily better for modelling vibrations of prestressed cable structures where the cable segments remain taut (due to initial prestress) at all times.

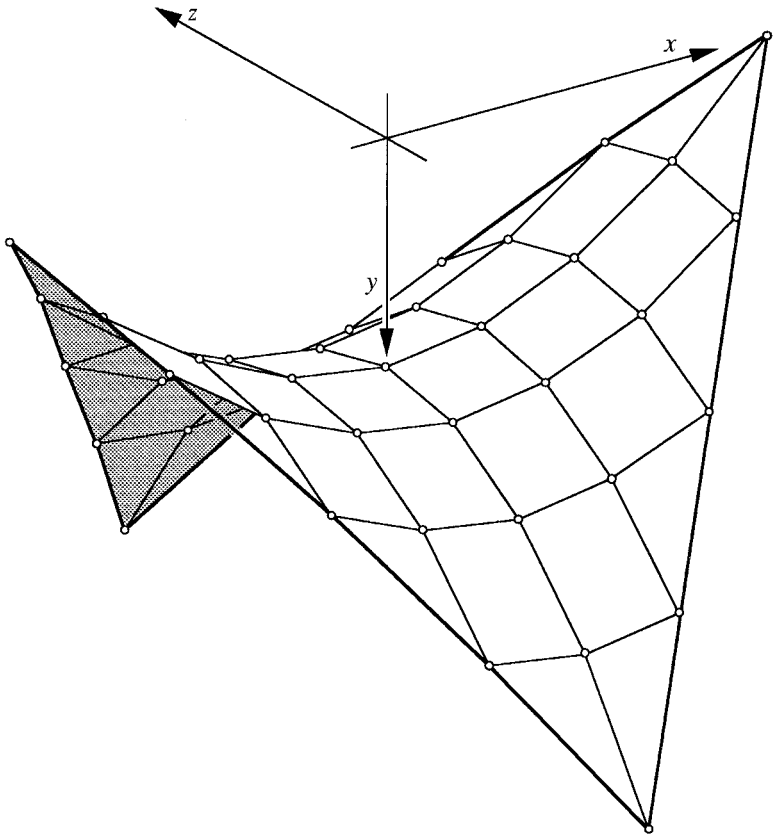


Fig. 8. The Aden Airways hyperbolic paraboloid.

Table 5
Table of natural frequencies (in rad/s) for the Aden Airways building (Fig. 8) using both lumped mass and distributed mass models

| Mass | Geshwinder and West, lumped | Swaddiwudhipong, lumped | Chisalita, lumped | Present study, lumped | Chisalita, distributed | Present study, distributed |
|---|---|---|---|---|---|---|
| $\omega_1$ | 32.87 | 32.57 | 32.892 | 32.890 | 36.945 | 36.473 |
| $\omega_2$ | 39.18 | 38.82 | 39.209 | 39.203 | 46.775 | 45.211 |
| $\omega_3$ | 39.89 | 39.50 | 39.916 | 39.909 | 50.343 | 46.432 |
| $\omega_4$ | 41.29 | 40.90 | 41.326 | 41.315 | 55.140 | 49.411 |
| $\omega_5$ | 43.81 | 43.39 | ⋮ | 43.837 | ⋮ | 53.634 |
| ⋮ | ⋮ | | ⋮ | ⋮ | ⋮ | ⋮ |
| $\omega_{75}$ | 1436 | | 1435.893 | 1435.896 | 2285.769 | 15733 |

## References


[1] ASCE Subcommittee. Cable-suspended roof construction state-of-the-art. ASCE J Struc Div 1971;97:715–1761.

[2] Chisalita A. Finite deformation analysis of cable networks. ASCE J Engng Mech 1984;110(2):207–23.

[3] Gambhir ML, Batchelor BdeV. A finite element for 3-D prestressed cablenets. Int J Numer Meth Engng 1977;11:1699–718.

[4] Gambhir ML, Batchelor BdeV. Finite element study of the free vibration of 3-D cable networks. Int J Solids Struct 1979;15:127–36.

[5] Geshwinder LF, West HH. Parametric investigations of vibrating cable networks. ASCE J Struct Div 1979;105(ST3):465–79.

[6] Jensen JJ. ine Statische und Dynamische Untersuchung der Seilund Membrantragwerke, Report No 70-1, Norwegian Institute of Technology, University of Trondheim, 1970.

[7] Knudson WC. Recent advances in the field of long span tension structures. Engng Struct 1991;13:164–77.

[8] Knudson WC. Static and dynamic analysis of cable-net structures. Ph.D. Thesis, University of California at Berkeley, CA, 1971.

[9] Kwan ASK, A new approach to geometric nonlinearity of cable structures, Computers & Structures 1998;67:243–52.

[10] Leonard JW. Non-linear dynamics of curved elements. ASCE J Engng Mech Div 1973;99:616–21.

[11] Morris NF. Dynamic response of cable networks. J Struct Div ASCE 1974;100(ST10):2091–108.

[12] Ozdemir H. A finite element approach for cable problems. Int J Solids Struct 1979;15:427–37.

[13] Sangster KG. Dynamic response of cable networks. Ph.D. Thesis, Queen's University, Kingston, Canada, 1974.

[14] Sangster KG, Batchelor BdeV. Non-linear dynamics analysis of 3-D cablenets. In: Proceedings of International Conference on Computational Methods in Non-linear Mechanics, University of Texas, 1974. p. 301–10.

[15] Shore S, Chaudhari B. Free vibration of cable networks utilizing analogous membranes. In: Proceedings of 9th International Congress of the Association of Bridges and Structural Engineering, Amsterdam. 1972, p. 445–51.

[16] Soler AI, Afshari H. On the analysis of cable network vibrations using Galerkin's method. ASME J Appl Mech 1970;37:606–11.

[17] Swaddiwudhipong S, Wang CM, Liew KM, Lee SL. Optimal pretensioned forces for cable networks. Computers & Structures 1989;33(6):1349–454.